

Chevkinite-group minerals from Russia and Mongolia: new compositional data from metasomatites and ore deposits

R. MACDONALD^{1,2,*}, B. BAGIŃSKI¹, P. KARTASHOV³, D. ZOZULYA⁴ AND P. DZIERŻANOWSKI¹

¹ IGMiP Faculty of Geology, University of Warsaw, 02-089 Warsaw, Poland

² Environment Centre, Lancaster University, Lancaster LA1 4YQ, UK

³ Institute of Ore Deposits, Russian Academy of Sciences, Moscow 109107, Russia

⁴ Geological Institute, Kola Science Centre, Russian Academy of Sciences, Apatity, Russia

[Received 21 November 2011; Accepted 1 March 2012; Associate Editor: Edward Grew]

ABSTRACT

Electron-microprobe analyses of Russian and Mongolian chevkinite-group minerals from little-known host lithologies, including various metasomatic rocks, quartzolites and an apatite deposit, are presented. The mineral species analysed include chevkinite-(Ce), perrierite-(Ce), polyakovite-(Ce) and Sr- and Zr-rich perrierite-(Ce). Compositional variation in the Sr-rich members of the group is broadly represented by the exchange vector $(\text{Fe} + \text{Mn} + \text{Al} + \text{REE}) \leftrightarrow (\text{Ca} + \text{Sr} + \text{Ti} + \text{Zr})$. Despite the varied parageneses, the chevkinite-(Ce) compositions are similar to previously published data. Many crystals have strong internal compositional variations, partly produced during primary crystallization and partly during low-temperature hydrothermal alteration.

KEYWORDS: chevkinite group, electron microprobe, intra-crystalline variations, hydrothermal alteration, chevkinite-(Ce), perrierite-(Ce), polyakovite-(Ce).

Introduction

CHEVKINITE-GROUP minerals (CGMs) are being recognized increasingly as accessory phases in a wide range of igneous and metamorphic rocks (Macdonald and Belkin, 2002; Belkin *et al.*, 2009; Macdonald *et al.*, 2009). Ten members of the group have been approved by the Commission of New Minerals, Nomenclature and Classification of the International Mineralogical Association (CNMNC IMA) (Table 1) and there are several potentially new species [e.g. ‘perrierite-(Ca)’ (Carlier and Lorand, 2008) and ‘perrierite-(Y)’ (Belkin *et al.*, 2009)]. One objective of ongoing research is to document the compositional

variation in the group and how this relates to mode of occurrence. Here we present the compositions of CGMs from a variety of Russian and Mongolian localities, with the following specific objectives: (1) to present new compositional data for CGMs in lithologies for which few data are available, including ore deposits, quartzolites and various metasomatic rocks; (2) to provide further compositional data on polyakovite-(Ce) from the type locality; (3) to describe the nature of intra-grain compositional variations and briefly examine the effects of probable hydrothermal alteration on certain CGMs, as previously described by Jiang (2006) and Vlach and Gualda (2007).

Samples

The Keivy peralkaline granite complex (2670–2610 Ma) is one of a suite of peralkaline

* E-mail: r.macdonald@lancaster.ac.uk
DOI: 10.1180/minmag.2012.076.3.06

TABLE 1. Members of the chevkinite group, accepted by the CNMNC-IMA.

Mineral	Ideal formula	Reference
Chevkinite subgroup		
Chevkinite-(Ce)	$(REE,Ca)_4Fe^{2+}(Ti,Fe^{3+},Fe^{2+},Al)_2Ti_2Si_4O_{22}$	Ito and Arem (1971)
Polyakovite-(Ce)	$(REE,Ca)_4(Mg,Fe^{2+})(Cr,Fe^{3+})_2(Ti,Nb)_2Si_4O_{22}$	Popov <i>et al.</i> (2001)
Maoniupingite-(Ce)	$(REE,Ca)_4(Fe^{3+},Ti,Fe^{2+},\square)(Fe^{3+},Fe^{2+},Nb,Ti)_2Ti_2Si_4O_{22}$	Shen <i>et al.</i> (2005)
Dingdaohengite-(Ce)	$Ce_4Fe^{2+}Ti_2Ti_2(Si_2O_7)_2O_8$	Xu <i>et al.</i> (2008)
Perrierite subgroup		
Perrierite-(Ce)	$(REE,Ca)_4Fe^{2+}(Ti,Fe^{3+},Fe^{2+},Al)_2Ti_2Si_4O_{22}$	Ito and Arem (1971)
Strontiochevkinite	$(Sr_2[La,Ce]_{1.5}Ca_{0.5})_4Fe_{0.5}^{2+}Fe_{0.5}^{3+}(Ti,Zr)_2Si_4O_{22}$	Haggerty and Mariano (1983)
Rengeite	$Sr_4ZrTi_4Si_4O_{22}$	Miyajima <i>et al.</i> (2001)
Matsubaraita	$Sr_4Ti_5(Si_2O_7)_2O_8$	Miyajima <i>et al.</i> (2002)
Hezuolinite	$(Sr,REE)_4Zr(Ti,Fe)_4Si_4O_{22}$	Yang <i>et al.</i> (2011)
Perrierite-(La)	$(La,Ce,Ca)_4(Fe^{2+},Mn)(Ti,Fe^{3+},Al)_4(Si_2O_7)_2O_8$	Chukanov <i>et al.</i> (2011)

granites, nepheline syenites and massif-type anorthosites in the Archaean Keivy terrane of the northeast Baltic Shield (Zozulya *et al.*, 2005). We have analysed CGMs from three types of occurrence within the complex, related to peralkaline granite and late, post-magmatic fluids, viz. a metasomatite in basic country rocks (sample 160b/620), quartzolites (sample PB-176 in gneissic country rock and samples 1/93 and 131/85 from the apical parts of granitic bodies) and a pegmatite (sample 5745b). Sample K3 is from borehole DH# 597, at a depth of 778.8 m, Umbozero lake, at the eastern contact of the Khibiny massif, where it occurs in a metasomatite. The type locality for the Cr-rich CGM polyakovite-(Ce) is in the Ilmen mountains, southern Urals. It was found in a dolomite veinlet cross-cutting phlogopite-olivine rock (Popov *et al.*, 2001). Specimen K2 is a cotyple from that locality. We have also analysed a CGM (sample K4) from a syenite pegmatite in vein 35, Vishnevye mountains, Chelyabinsk Oblast', which is also in the southern Urals.

Portnov (1964) described a perrierite that was rich in Sr and Zr from aegirized syenite pegmatites in the Burpala massif. This phase (sample BP) is of particular interest because it is, in some respects, compositionally transitional between perrierite and rengerite and broadly related to hezuolinite (Table 1). Andreev and Ripp (1995) gave a composition of perrierite-(Ce) from the Apatitovye deposit in the Mushugai-Khuduk carbonatite complex, Gobi desert, Mongolia, which contained unusually large

amounts of Ca (8.43 wt.% CaO) and Ba (2.06 wt.% BaO). It is difficult to calculate a stoichiometric and charge-balanced formula from their compositional data and therefore, a redetermination (on sample K1, which is from the same specimen) was considered useful. The CGM samples K6, K7 and K8 are from epidote-quartz metasomatites in the western ore zone of the Khaldzan-Buragtag massif, Mongolia. Sample K9 is from the trench Probe TsKh-90-III, 'Point 2300', at the northernmost part of the western ore zone, and K10 is from trench 4, in the western ore zone.

Further locality and sample details are provided in Table 2 and as supplementary material which has been deposited with the Principal Editors of *Mineralogical Magazine* and is available at www.minersoc.org/pages/e_journals/dep_mat.html.

Analytical methods and site allocations

The CGM compositions were determined by electron-microprobe analysis at the Inter-Institute Analytical Complex at the IGMiP Faculty of Geology, University of Warsaw, using a Cameca SX-100 microprobe equipped with four wavelength-dispersive spectrometers. The accelerating voltage was 15 kV and the probe current was 20 nA. Counting times were 20 s on peak and 10 s on each of two background positions. The standards, crystals and X-ray lines used and detection limits are listed in Table 3. The 'PAP' $\phi(\rho Z)$ program (Pouchou and Pichoir, 1991) was used to reduce the data. Representative composi-

CHEVKINITE-GROUP MINERALS

TABLE 2. Details of the locations, host lithology and associated species for the investigated samples.

Sample	Locality	Mineral	Host rock	Associated minerals
160b/62	Keivy, El'ozero	chevkinite-(Ce)	metasomatite	q, alb, mcl, aeg, Na-ab, ann, z, th, all, ferg, gad, pyr, fl, cass, crich, danalite, monazite
PB-176	Keivy, Rova	chevkinite-(Ce)	quartzolite	q, alb, arfv, aeg, ann, mt, ilm, z, ferg, brith-(Ce), bast, thor, fl
1/93	Keivy, Rova	chevkinite-(Ce)	quartzolite	q, mcl, aeg, arfv, mt, ilm, fl, z, ferg, brith-(Y), ytrr, thor, aesch-(Ce)
131/85	Keivy, Pessarjok	chevkinite-(Ce)	quartzolite	q, mcl, aeg, arfv, fl, mt, ilm, z, ferg, brith-(Y) thor, ytrr
5745b	Keivy, Purnach	chevkinite-(Ce)	pegmatite	q, mcl, alb, aeg, mt, ferg, brith-(Y), gad, aesch-(Y)
K3	Kola, Khibiny	chevkinite-(Ce)	metasomatite	kat, neph, K-f, mt, z, pyr, chalc
K2	Urals, Ilmen Mts	polyakovite-(Ce)	dolomite vein	flrich, thorianite, Th-niobate
K4	Urals, Vishnevye	chevkinite-(Ce)	pegmatite	alteration rim of bast, ilm
BP	Burpala massif	Sr- and Zr-rich perrierite-(Ce)	pegmatite	aeg, pyr, Ca-cat, tit, z
K1	Mongolia, Mushugai	perrierite-(Ce)	apatite ore	apatite, cpx, biot, K-fs, garnet, mt
K6	Mongolia, Khaldzan	chevkinite-(Ce)	ores associated with metasomatites	epid, q, act, ferg, z, all
K7	Mongolia, Khaldzan	chevkinite-(Ce)	ores associated with metasomatites	epid, q, act, ferg, z, all
K8	Mongolia, Khaldzan	chevkinite-(Ce)	ores associated with metasomatites	epid, q, act, ferg, z, all
K9	Mongolia, Khaldzan	chevkinite-(Ce)	ores associated with metasomatites	ferg, columbite, z, epid, all
K10	Mongolia, Khaldzan	chevkinite-(Ce)	ores associated with metasomatites	alteration rim of titan, fersmite, all

Abbreviations are as follows: act, actinolite; aeg, aegirine; aesch, aeschynite; alb, albite; all, allanite; ann, annite; arfv, arfvedsonite; bast, bastnäsite; biot, biotite; brith, britholite; Ca-cat, Ca-catapleite; cass, cassiterite; chalc, chalcopyrite; cpx, clinopyroxene; crich, crichtonite; epid, epidote; ferg, fergusonite; fl, fluorite; flrich, fluorichterite; gad, gadolinite; ilm, ilmenite; kat, kataphorite; K-f, K-feldspar; mcl, microcline; mt, magnetite; Na-ab, sodic amphibole; neph, nepheline; pyr, pyrite; q, quartz; thor, thorite; titan, titanite; ytrr, yttrialite; z, zircon.

TABLE 3. Analytical details.

Element	Line	Crystal	Standard	Approximate detection limit (wt.%)
Al	<i>K</i> α	TAP	orthoclase	0.008
Ba	<i>L</i> α	LiF	baryte	0.114
Ca	<i>K</i> α	PET	CaSiO ₃	0.008
Ce	<i>K</i> α	PET	CeP ₅ O ₁₄	0.053
Dy	<i>L</i> β	LiF	<i>REE1</i> *	0.312
Eu	<i>L</i> β	LiF	<i>REE2</i> *	0.263
Fe	<i>K</i> α	LiF	hematite	0.034
Gd	<i>L</i> β	LiF	GdP ₅ O ₁₄	0.126
Hf	<i>M</i> α	TAP	Hf-SPI	0.033
La	<i>L</i> α	PET	LaB ₆	0.052
Mg	<i>K</i> α	TAP	diopside	0.006
Mn	<i>K</i> α	LiF	rhodonite	0.036
Na	<i>K</i> α	TAP	albite	0.012
Nb	<i>L</i> α	PET	Nb metal	0.054
Nd	<i>L</i> β	LiF	NdP ₅ O ₁₄	0.121
P	<i>K</i> α	PET	Apatite Jap2	0.014
Pr	<i>L</i> β	LiF	PrP ₅ O ₁₄	0.119
Sc	<i>K</i> α	PET	Sc metal	0.010
Si	<i>K</i> α	TAP	CaSiO ₃	0.006
Sm	<i>L</i> β	LiF	SmP ₅ O ₁₄	0.115
Sr	<i>L</i> α	TAP	SrTiO ₃	0.027
Ta	<i>M</i> α	TAP	Ta metal	0.036
Tb	<i>L</i> α	LiF	<i>REE4</i> *	0.144
Th	<i>M</i> α	PET	ThO ₂ synthetic	0.086
Ti	<i>K</i> α	PET	rutile	0.016
U	<i>M</i> β	PET	vorlanite (CaUO ₄)	0.077
Y	<i>L</i> α	TAP	Y ₃ Al ₅ O ₁₂	0.028
Yb	<i>L</i> α	LiF	<i>REE3</i> *	0.136
Zr	<i>L</i> α	PET	Zircon ED2	0.051

* The codes *REE1*–*4* refer to glasses containing *REE* (*REEPO*₄) (Jarosewich and Boatner, 1991).

tional data and formulae are listed in Tables 4–7; the full data set is given in Supplementary Table 1, which has been deposited with the Principal Editors of *Mineralogical Magazine* and is available at www.minersoc.org/pages/e_journals/dep_mat.html.

In the majority of cases, the cation sum in our compositions is in the range 13.0–13.3, which we consider to be of acceptable quality for CGMs, especially as the sums would be reduced if some Fe²⁺ were recalculated as Fe³⁺. The oxide totals are >97 wt.% in most cases but some are as low as 95 wt.%. The low totals are probably due to secondary hydration, particularly in Keivy samples 160b/62 and 1/93, which are mantled by what we interpret as hydrothermally altered rims.

The general formula for chevkinite and perrierite can be written $A_4BC_2D_2Si_4O_{22}$, where

$A = \text{Ca, Sr, REE, Th}$; $B = \text{Fe}^{2+}$; $C = \text{Fe}^{2+}, \text{Fe}^{3+}, \text{Ti}$, Al, Mg, Mn; and $D = \text{Ti, Nb}$. The majority of our compositional data are in excellent agreement with this formula, including the Sr- and Zr-rich perrierite-(Ce) from the Burpala massif (Tables 4 and 5; Supplementary Table 1). The general formula is more difficult to apply to the most Sr-rich minerals in the perrierite subgroup; Miyajima *et al.* (2001), for example, give an ideal formula of Sr₄ZrTi₄Si₄O₂₂ for rengenite and Miyajima *et al.* (2002) list matsubaraitite as Sr₄Ti₅(Si₂O₇)₂O₈.

General geochemical features

Haggerty and Mariano (1983) suggest that the most diagnostic difference between chevkinite and perrierite is the β angle (~100° and ~113°,

CHEVKINITE-GROUP MINERALS

TABLE 4. Representative compositions (in wt.%) of chevkinite-group minerals from Russia.

Specimen	Chevkinite-(Ce)					K3	K4	K2 Polyakovite	BP Perrierite-(Ce)
	160b/62	PB-176	1/93	131/85	5745b				
Nb ₂ O ₅	0.55	1.50	0.99	1.10	0.61	3.39	2.18	4.36	0.28
Ta ₂ O ₅	0.15		0.10				0.20		0.08
P ₂ O ₅	b.d.	b.d.	0.06	b.d.	b.d.	b.d.	b.d.	0.04	b.d.
TiO ₂	16.51	16.25	15.94	17.34	17.32	15.39	15.63	9.55	21.82
ZrO ₂	0.02	0.15	0.07	0.22	b.d.	0.27	0.20	b.d.	4.96
ThO ₂	0.54	0.67	2.43	1.27	1.36	0.64	2.76	2.45	0.50
UO ₂	b.d.	b.d.	b.d.	b.d.	0.15	b.d.	b.d.	b.d.	b.d.
SiO ₂	18.77	18.74	18.66	20.24	18.40	18.75	19.02	18.43	20.01
Al ₂ O ₃	0.78	0.19	0.06	0.03	0.05	0.06	0.17	0.06	0.18
Cr ₂ O ₃								8.01	
La ₂ O ₃	13.62	9.13	9.58	10.63	10.07	15.50	16.40	16.13	14.14
Ce ₂ O ₃	23.02	20.24	20.58	20.67	20.86	22.18	20.94	23.85	15.33
Pr ₂ O ₃	1.83	2.21	2.35	2.23	2.64	1.79	1.31	2.00	0.91
Nd ₂ O ₃	6.05	8.46	7.63	8.01	8.52	4.73	3.42	4.98	1.62
Sm ₂ O ₃	0.82	1.21	1.33	1.22	1.29	0.26	b.d.	0.24	0.25
Gd ₂ O ₃	0.61	0.59	1.08	0.82	0.90	0.21	b.d.	0.23	0.24
Dy ₂ O ₃	b.d.	0.51	b.d.	b.d.	0.47	b.d.	b.d.	b.d.	b.d.
Yb ₂ O ₃	b.d.	0.22	b.d.	b.d.	b.d.	b.d.	b.d.	b.d.	b.d.
Y ₂ O ₃	0.47	1.77	1.21	0.99	1.44	0.21	0.04	0.21	b.d.
FeO*	10.87	11.59	12.37	11.05	11.48	11.74	11.29	4.56	6.10
MnO	0.21	0.57	0.36	0.29	0.34	0.42	0.91	0.04	0.89
MgO	0.17		b.d.	b.d.	b.d.	0.08	0.22	2.17	0.06
CaO	1.49	2.49	1.34	1.71	1.33	2.09	2.82	0.84	2.17
SrO	0.09	0.14	0.14	0.19	0.13	0.75		0.53	8.05
BaO	0.16		0.13						0.27
Na ₂ O	b.d.	b.d.	b.d.	0.06	b.d.	b.d.	b.d.	b.d.	0.33
Total	96.79	96.78	96.68	98.53	97.51	98.68	97.72	98.68	98.47

Blank is not determined; b.d. is below detection limit.

Sample locations are as follows: 160b/62, El'ozero, West Keivy; PB-176 and 1/93, Rova, West Keivy; 131/85, Pessarjok, West Keivy; 131/85 Pessarjok, West Keivy; 5745b, Purnach massif, Keivy; K3, Khibiny massif, Kola; K4, Vishnevy mountains, Urals; K2, Ilmen mountains, Urals; BP, Burpala massif, north Baikal.

* FeO with all Fe as Fe²⁺.

respectively), which is related to different cation–oxygen bond length patterns in their structures. All subsequent structural studies have confirmed this difference between the chevkinite and perrierite subgroups. In the absence of structural data, Macdonald and Belkin (2002) proposed the use of an empirical discrimination diagram based on FeO* vs. CaO contents, and this was modified by Macdonald *et al.* (2009) to FeO* vs. (CaO + SrO), to include more Sr-rich minerals. Despite the simplicity of the discrimination, it has proved remarkably robust in separating CGMs with $\beta \sim 100^\circ$ (the chevkinite subgroup) from those with $\beta \sim 113^\circ$ (the perrierite subgroup); we know of no structurally-determined example (published since

2002) that has not been classified in the correct subgroup using this type of diagram. New data from this study are plotted as averages and fields in Fig. 1. Minerals from two localities (Apatitovye and Burpala) belong to the perrierite subgroup, all others to the chevkinite subgroup.

Polyakovite

Our new compositional data for polyakovite-(Ce) are similar to those of Popov *et al.* (2001), with slightly higher Cr₂O₃ and Nb₂O₅, and lower SiO₂, FeO*, MgO, CaO and La₂O₃. We report a small but significant Sr content (0.06 a.p.f.u.). The formula determined by Popov *et al.* (2001) used

TABLE 5. Structural formulae of chevkinite-group minerals from Russia.

Specimen	160b/62	PB-176	1/93	131/85	5745b	K3	K4	K2	BP
	Chevkinite-(Ce)						Polyakovite		Perrierite-(Ce)
Ca	0.346	0.576	0.315	0.385	0.310	0.479	0.648	0.195	0.465
Sr	0.011	0.018	0.018	0.023	0.016	0.093		0.067	0.933
Ba	0.014		0.011						0.021
Na	0.000	0.000	0.000	0.024	0.000	0.000	0.000	0.000	0.128
La	1.089	0.727	0.775	0.824	0.807	1.224	1.297	1.290	1.043
Ce	1.827	1.600	1.653	1.590	1.659	1.738	1.643	1.894	1.122
Pr	0.145	0.174	0.188	0.171	0.209	0.140	0.102	0.158	0.066
Nd	0.468	0.652	0.598	0.601	0.661	0.362	0.262	0.386	0.116
Sm	0.061	0.090	0.101	0.088	0.097	0.019	0.000	0.018	0.017
Gd	0.044	0.042	0.079	0.057	0.065	0.015	0.000	0.017	0.016
Dy	0.000	0.035	0.000	0.000	0.033	0.000	0.000	0.000	0.000
Yb	0.000	0.014	0.000	0.000	0.000	0.000	0.000	0.000	0.000
Y	0.054	0.203	0.141	0.111	0.166	0.024	0.005	0.024	0.000
Th	0.027	0.033	0.121	0.061	0.067	0.031	0.135	0.121	0.023
U	0.000	0.000	0.000	0.000	0.007	0.000	0.000	0.000	0.000
Sum A	4.086	4.165	4.000	3.935	4.098	4.125	4.091	4.170	3.951
Fe ²⁺	1.000	1.000	1.000	1.000	1.000	1.000	1.000	0.827	1.000
Mn	0.000	0.000	0.000	0.000	0.000	0.000	0.000	0.007	0.000
Mg	0.000	0.000	0.000	0.000	0.000	0.000	0.000	0.166	0.000
Sum B	1.000	1.000	1.000	1.000	1.000	1.000	1.000	1.000	1.000
Fe ²⁺	0.970	1.092	1.270	0.942	1.086	1.101	1.024	0.000	0.020
Mn	0.039	0.104	0.067	0.052	0.063	0.076	0.165	0.000	0.151
Mg	0.055		0.000	0.000	0.000	0.026	0.070	0.535	0.018
Nb	0.054	0.146	0.098	0.104	0.060	0.328	0.211	0.000	0.025
Ta	0.009		0.006				0.012		0.004
Zr	0.002	0.016	0.007	0.023	0.000	0.028	0.021	0.000	0.484
Al	0.199	0.048	0.016	0.007	0.013	0.015	0.043	0.015	0.042
Cr								1.374	
Ti	0.691	0.638	0.630	0.740	0.830	0.477	0.519	0.000	1.281
Sum C	2.019	2.045	2.094	1.868	2.051	2.051	2.065	1.924	2.026
Ti	2.000	2.000	2.000	2.000	2.000	2.000	2.000	1.558	2.000
Nb	0.000	0.000	0.000	0.000	0.000	0.000	0.000	0.428	0.000
Sum D	2.000	2.000	2.000	2.000	2.000	2.000	2.000	1.986	2.000
P	0.000	0.000	0.011	0.000	0.000	0.000	0.000	0.007	0.000
Si	4.068	4.045	4.094	4.252	3.997	4.013	4.076	3.997	4.001
Sum T	4.068	4.045	4.105	4.252	3.997	4.013	4.076	4.004	4.001
Σ cations	13.2	13.3	13.2	13.1	13.1	13.2	13.2	13.1	13.0

Formulae are based on 22 oxygen atoms.

Sample locations are as follows: 160b/62, El'ozero, West Keivy; PB-176 and 1/93, Rova, West Keivy; 131/85, Pessarjok, West Keivy; 131/85 Pessarjok, West Keivy; 5745b, Purnach massif, Keivy; K3, Khibiny massif, Kola; K4, Vishnevy mountains, Urals; K2, Ilmen mountains, Urals; BP, Burpala massif, north Baikal.

CHEVKINITE-GROUP MINERALS

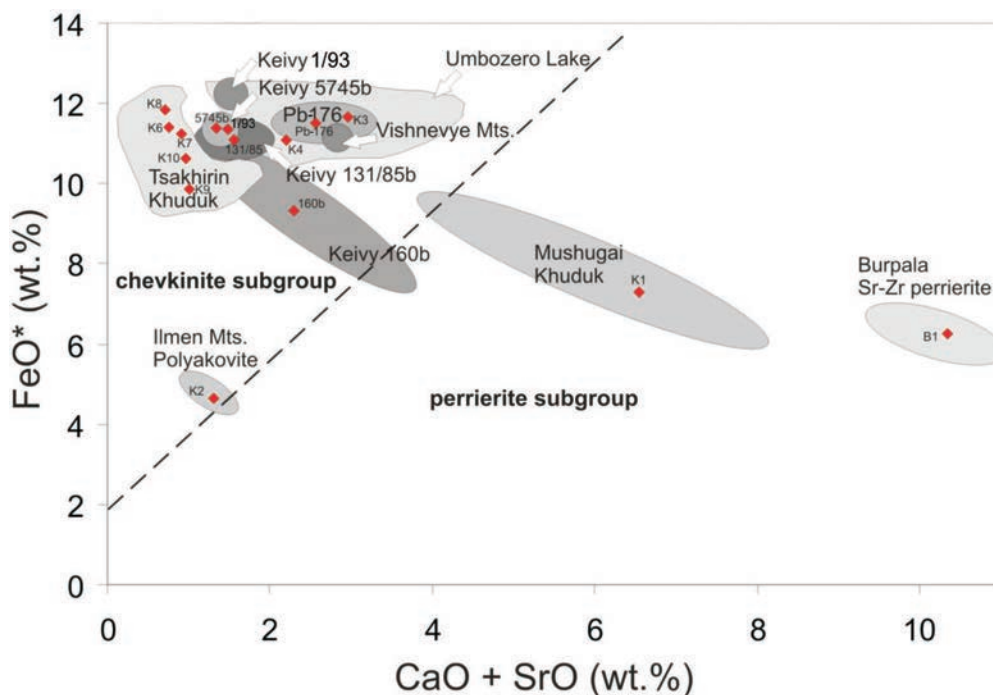


FIG. 1. An empirical FeO^* vs. $(\text{CaO} + \text{SrO})$ diagram, which can be used to discriminate between minerals of the chevkinite and perrierite subgroups (Macdonald *et al.*, 2009). The FeO^* is total Fe expressed as Fe^{2+} . New CGM data are shown as averages and fields (with full data in Supplementary Table 1a,b).

an $\text{Fe}^{2+}/\text{Fe}^{3+}$ ratio determined by Mössbauer spectroscopy on a sample annealed in a helium atmosphere. Using the same ratio, our composition can be written: $(\text{Ce}_{1.87}\text{La}_{1.27}\text{Nd}_{0.37}\text{Pr}_{0.14}\text{Sm}_{0.02}\text{Gd}_{0.02}\text{Y}_{0.02}\text{Ca}_{0.19}\text{Sr}_{0.06}\text{Th}_{0.12})_{4.10}(\text{Mg}_{0.69}\text{Fe}_{0.18}\text{Fe}_{0.05}^{3+})_{0.92}(\text{Cr}_{1.37}\text{Fe}_{0.60}^{3+})_{1.97}(\text{Ti}_{1.52}\text{Nb}_{0.44})_{1.96}(\text{Si}_{3.93}\text{Al}_{0.02})_{3.95}\text{O}_{22}$.

This is very similar to the formula reported by Popov *et al.* (2001) (Table 1). The dominance of Mg in the *B* site and of Cr in the *C* site, features not previously reported in CGMs, and the significant Nb content in the *D* site are notable.

The only other report of polyakovite (as ‘Cr-chevkinite’) is as inclusions in diamonds from the River Ranch kimberlite pipe in Zimbabwe (Kopylova *et al.*, 1997). This phase has a higher Cr content than the Russian material (1.95 a.p.f.u.) and Cr is the sole occupant of the *C* site. It also has higher Sr and Al contents, lower Fe, Th and Nb contents, and a lower La/Ce ratio. Given the very different parageneses of the Russian and Zimbabwean minerals, it is probable that other Cr-rich CGMs remain to be recognized.

Perrierite from Apatitovye

Our data confirm that the phase from the Apatitovye ore deposit (Andreev and Ripp, 1995) is perrierite-(Ce) but with lower Ca (6.16 wt.% CaO) and Ba (below the detection limit of 0.13 wt.% BaO) contents than in their analysis. We suspect that the high BaO in their wet-chemical analysis was a result of admixture with barium carbonates, which Andreev and Ripp (1995) reported in these samples. The relatively high levels of Al (2.35 wt.% Al_2O_3), Mg (0.84 wt.% MgO) and Zr (2.41 wt.% ZrO_2) are common in perrierite (Macdonald and Belkin, 2002; Macdonald *et al.*, 2009).

Strontium- and zirconium-rich perrierite from Burpala

Our data for the strontium- and zirconium-rich perrierite from Burpala is generally similar to those of Portnov (1964), the only major difference being that we found Y to be below the instrumental

detection limit, whereas he reported 0.90 wt.% Y_2O_3 . Our formula is $(Ce_{1.13}La_{1.05}Sr_{0.95}Ca_{0.50}Na_{0.14}Nd_{0.12}Pr_{0.07})_{3.96}Fe^{2+}(Ti_{1.36}Zr_{0.48}Mn_{0.16}Fe_{0.06}Mg_{0.02})_{2.08}Ti_2(Si_{3.92}Al_{0.04})_{3.96}O_{22}$. The relatively high La/Ce ratio (0.93), the low *MREE* and *HREE* content, and the very low Fe in the *C* site, which is dominated by Ti, are notable.

Strontium-rich members (taken here to have $SrO > 2$ wt.%) of the perrierite subgroup have been reported from at least seven localities, but there are insufficient analytical data to propose compositional boundaries as yet, e.g. between hezuolinite (Table 1) and Sr-bearing perrierite-(Ce) (Tables 4 and 5). However, compositional variation in the Sr-rich phases is fairly well represented by the exchange $(Fe + Mn + Al + REE) \leftrightarrow (Ca + Sr + Ti + Zr)$, although charges are not balanced (Fig. 2). In the transition from perrierite to rengerite and matsubaraite, *REE* are generally replaced by Ca + Sr (with increasing Sr/Ca ratios), and M^{2+} and M^{3+} cations by Ti or Zr.

Keivy, Khibiny, Urals, Khaldzan-Buragtag

The CGMs from Keivy, Khibiny, the Urals and Khaldzan-Buragtag are broadly similar compositionally. They are chevkinite-(Ce) (Fig. 1), which

is rather low in Ca + Sr (< 0.6 a.p.f.u.), and with notably low Zr (≤ 0.11 a.p.f.u.), Al (≤ 0.12 a.p.f.u.) and Th (≤ 0.16 a.p.f.u.) contents. The niobium contents are low (≤ 0.46 a.p.f.u.). On a *REE* vs. (Ca + Sr) plot, all of the compositions are close to the *REE* axis (Fig. 3). In two samples, Ti_C exceeds Fe_C ; otherwise, $Fe_C > Ti_C$. Some minor constituents show significant differences between samples. For example, Nb_2O_5 ranges from 0.61–3.32 wt.% and ZrO_2 from 0.04–0.45 wt.% (Tables 4–7). Total *REE* are in the limited range 3.4–4.0 a.p.f.u. but the relative proportions are variable; La/Ce and La/Y (atomic) are in the ranges 0.44–0.70 and 4.0–53, respectively. The samples with lowest La/Ce have the highest Nd values.

Whether the CGMs from the different parageneses in the Keivy massif (metasomatite, quartzolites and pegmatite) would have different compositions to CGMs from other parageneses, and to each other, was of particular interest. We found that none of the Keivy samples was in any way compositionally unusual compared to published compositions of chevkinite-(Ce) (see compilations in Macdonald and Belkin, 2002; Vlach and Gualda, 2007; Macdonald *et al.*, 2009).

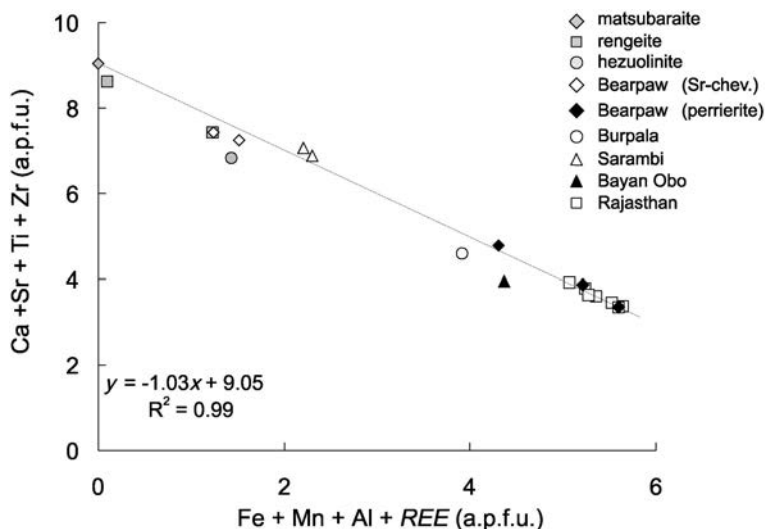


FIG. 2. Compositional variation in the Sr-rich members ($SrO > 2$ wt.%) of the perrierite subgroup. Data sources are as follows: Sr- and Zr-rich perrierite-(Ce), Burpala massif, this paper; strontio-chevkinite and perrierite-(Ce), Bearpaw mountains (Chakhmouradian and Mitchell, 1999); rengerite, Japan, (Miyajima *et al.*, 2001); matsubaraite, Japan (Miyajima *et al.*, 2002); strontio-chevkinite, Sarambi, Paraguay (Haggerty and Mariano, 1983); Bayan Obo, China (Shimazaki *et al.*, 2008); hezuolinite, Saima complex, China (Yang *et al.*, 2011); Rajasthan, India (Macdonald *et al.*, 2009).

CHEVKINITE-GROUP MINERALS

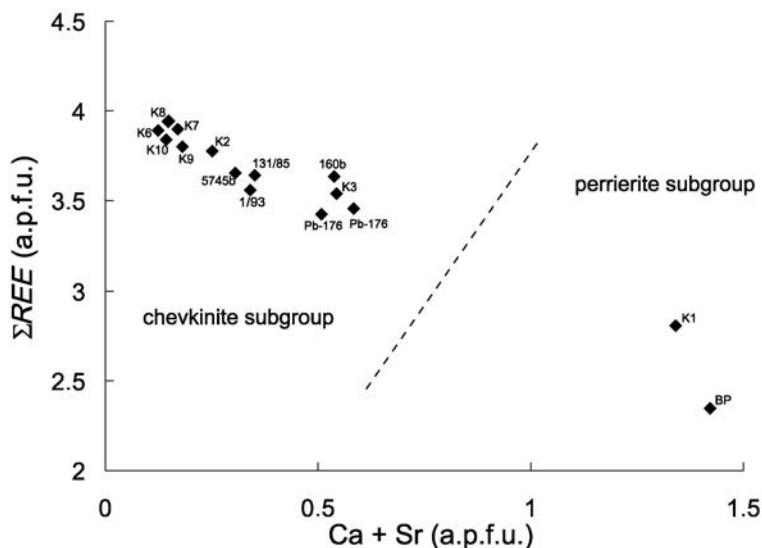


FIG. 3. A REE vs. (Ca + Sr) plot to show the Ca-poor (<0.2 a.p.f.u.) nature of certain Russian samples. For clarity, only average compositions are shown. The dashed line is the approximate boundary between phases of the chevkinite and perrierite subgroups. Samples 5745b, 131/85, 1/93, 160b/62 and Pb-176 are from the Keivy complex, Kola; K1, Mushugai-Khuduk complex, Mongolia; K2, polyakovite, Urals; K3, Khibiny massif, Kola; K4, Vishnevye mountains, Urals; K6, K7, K8, K9, K10, Khaldzan-Buragtag massif, Mongolia. Averages and the full dataset are in Supplementary Table 1.

Comparing the different parageneses, they can be divided into two slightly different groups: those from metasomate 160b/62 and quartzolite Pb-176 are rather more calcium-rich than those from the other occurrences (Fig. 1). For 160b/62, this is in keeping with the more basic environment of crystallization; Macdonald and Belkin (2002) noted that, in general, perrierite crystallizes from more basic magmas than chevkinite. For Pb-176 the higher Ca content might be explained by the incorporation of host gneissic material with a higher Ca content into the quartzolite.

Intra-crystalline variation

It is clear from Fig. 1 that although some chevkinite-(Ce) samples are compositionally fairly homogeneous (e.g. 5745b, 1/93), others have considerable intra-crystalline variation. Although details of the compositional variations differ from sample to sample, an overall negative correlation suggests the existence of two 'endmembers', one with a higher content of perrierite components (darker on the back-scattered electron images) and the other more chevkinitic (brighter on the back-scattered elec-

tron images). A similar situation was described by Macdonald *et al.* (2009) in perrierite-(Ce) from Roseland, Virginia. On the basis of data from metaluminous alkali-feldspar syenites and peralkaline alkali-feldspar granites of the A-type from Graciosa Province, Brazil, Vlach and Gualda (2007) proposed that compositional variation in the CGM can be expressed as:



Figure 4 shows that this relationship can be applied very successfully to our chevkinite-(Ce) dataset. Thus compositional differences within our crystals largely mirror those which have been identified more generally and they can be provisionally ascribed to temperature variation during magmatic crystallization.

Patchy zoning of the kind found here in the CGMs, with attendant strong compositional heterogeneity, is common in accessory phases. It has been recorded, for example, in minerals of the pyrochlore group (Lumpkin and Ewing, 1992, 1995, 1996), monazite (Townsend *et al.*, 2000), zircon (Wang *et al.*, 2003; Nasdala *et al.*, 2009, 2010; Gagnevin *et al.*, 2010), apatite (Harlov and Förster, 2003), fergusonite (Tomašić *et al.*, 2006;

TABLE 6. Representative compositions (wt.%) of chevkinite-group minerals from Mongolia.

Specimen	K1	K6	K7	K8	K9	K10
	Perrierite-(Ce)	Chevkinite-(Ce)				
Nb ₂ O ₅	0.11	3.01	2.01	1.93	1.73	2.63
Ta ₂ O ₅	0.13					
P ₂ O ₅	b.d.	0.03	b.d.	b.d.	b.d.	b.d.
TiO ₂	19.90	14.62	15.25	15.47	17.18	15.62
ZrO ₂	2.48	b.d.	b.d.	b.d.	0.21	0.46
ThO ₂	0.55	0.23	0.18	0.11	0.72	0.20
UO ₂	b.d.	b.d.	b.d.	b.d.	b.d.	b.d.
SiO ₂	20.89	18.15	18.31	18.56	18.33	18.37
Al ₂ O ₃	2.46	b.d.	b.d.	b.d.	b.d.	b.d.
La ₂ O ₃	12.63	10.86	12.85	13.46	10.45	10.55
Ce ₂ O ₃	18.97	23.76	23.94	24.34	23.14	23.35
Pr ₂ O ₃	1.27	2.95	2.80	2.48	2.75	2.89
Nd ₂ O ₃	3.84	9.74	8.57	8.26	9.47	8.94
Sm ₂ O ₃	0.39	1.19	0.67	0.56	1.51	1.32
Gd ₂ O ₃	b.d.	0.57	0.43	0.43	0.66	0.93
Dy ₂ O ₃	b.d.	b.d.	b.d.	b.d.	0.39	b.d.
Yb ₂ O ₃	b.d.	b.d.	b.d.	b.d.	b.d.	b.d.
Y ₂ O ₃	b.d.	0.18	0.20	0.14	0.52	0.51
FeO*	6.67	11.65	12.22	12.21	9.38	10.53
MnO	0.13	0.74	0.52	0.47	1.31	0.95
MgO	0.94	b.d.	b.d.	b.d.	b.d.	b.d.
CaO	7.17	0.31	0.68	0.64	0.21	0.32
SrO	0.34	0.44	0.06	0.11	0.39	0.61
Na ₂ O	b.d.	b.d.	b.d.	b.d.	0.20	0.18
Total	99.05	98.58	98.78	99.40	98.68	98.71

Blank is not determined; b.d. is below detection limit.

Sample locations are as follows: K1, Mushugai-Khuduk complex; K6 to K10 are from the western ore zone, Khaldzan-Buragtag massif, Altai mountains.

* FeO with all Fe as Fe²⁺.

Ruschel *et al.*, 2010) and chevkinite (Vlach and Gualda, 2007). Its formation has been ascribed to various processes including: (1) element mobility and recrystallization during metamictization, the process possibly being enhanced by fluids (Tomašić *et al.*, 2006); (2) recrystallization related to fluid influx(es) (Townsend *et al.*, 2000; Harlov and Förster, 2003); (3) diffusion-limited dissolution–recrystallization in response to magma mixing (Gagnevin *et al.*, 2010). Our data by themselves do not allow us to distinguish between these possibilities with any certainty and we are currently employing a combination of thermal, diffraction and spectroscopic methods in an attempt to identify the dominant process(es) in CGMs. However, we can comment on the question as to whether the compositional variability in the CGMs is a primary, syn-crystallization feature, or a later overprint.

Variability during primary crystallization

The degree of compositional homogeneity in primary magmatic phases may be assessed using phenocrysts in eruptive rocks, which are assumed to have been quenched relatively rapidly from magmatic temperatures and thus to have retained their high-temperature structure. We have data for perrierite-(Ce) from Nettuno, Italy, where Macdonald *et al.* (2009) determined three points on each of 20 grains, and a smaller set for chevkinite-(Ce) from the Lava Creek Tuff, Yellowstone, Wyoming, USA, where a total of 16 points was determined on two crystals (authors' unpublished data). In both cases, the major components, taken to have abundances ≥ 5 wt.%, show relative standard deviations $\leq 2\%$ (Ce₂O₃, FeO*, TiO₂, SiO₂) or between 2 and 6% (La₂O₃, Nd₂O₃, Al₂O₃, CaO). The lower values are close to the precision of the analytical

CHEVKINITE-GROUP MINERALS

TABLE 7. Structural formulae of chevkinite-group minerals from Mongolia.

Specimen	K1	K6	K7	K8	K9	K10
	Perrierite-(Ce)	Chevkinite-(Ce)				
Ca	1.478	0.073	0.160	0.149	0.049	0.075
Sr	0.038	0.056	0.008	0.014	0.049	0.077
Na	0.000	0.000	0.000	0.000	0.084	0.076
La	0.896	0.884	1.038	1.079	0.837	0.849
Ce	1.336	1.919	1.920	1.938	1.839	1.866
Pr	0.089	0.237	0.223	0.196	0.217	0.230
Nd	0.264	0.767	0.670	0.641	0.734	0.697
Sm	0.026	0.090	0.051	0.042	0.113	0.099
Gd	0.000	0.042	0.031	0.031	0.047	0.067
Dy	0.000	0.000	0.000	0.000	0.027	0.000
Yb	0.000	0.000	0.000	0.000	0.000	0.000
Y	0.000	0.021	0.023	0.016	0.060	0.059
Th	0.024	0.012	0.009	0.005	0.036	0.010
U	0.000	0.000	0.000	0.000	0.000	0.000
Sum A	4.151	4.101	4.134	4.113	4.092	4.106
Fe ²⁺	1.000	1.000	1.000	1.000	1.000	1.000
Mn	0.000	0.000	0.000	0.000	0.000	0.000
Mg	0.000	0.000	0.000	0.000	0.000	0.000
Sum B	1.000	1.000	1.000	1.000	1.000	1.000
Fe ²⁺	0.073	1.149	1.239	1.220	0.703	0.922
Mn	0.021	0.138	0.096	0.087	0.241	0.176
Mg	0.269	0.000	0.000	0.000	0.000	0.000
Nb	0.010	0.300	0.199	0.190	0.170	0.260
Ta	0.007				0.000	
Zr	0.233	0.000	0.000	0.000	0.022	0.049
Al	0.558	0.000	0.000	0.000	0.000	0.000
Ti	0.879	0.425	0.512	0.529	0.804	0.564
Sum C	2.049	2.012	2.047	2.026	1.940	1.970
Ti	2.000	2.000	2.000	2.000	2.000	2.000
Nb	0.000	0.000	0.000	0.000	0.000	0.000
Sum D	2.000	2.000	2.000	2.000	2.000	2.000
P	0.000	0.006	0.000	0.000	0.000	0.000
Si	4.018	4.003	4.011	4.035	3.978	4.009
Sum T	4.018	4.009	4.011	4.035	3.978	4.009
Σ cations	13.2	13.1	13.2	13.2	13.0	13.1

Formulae are based on 22 oxygen atoms.

Sample locations are as follows: K1, Mushugai-Khuduk complex; K6 to K10 are from the western ore zone, Khaldzan-Buragtag massif, Altai mountains.

techniques employed, estimated for Nettuno as 1–2% for oxide concentrations >1 wt.% (Macdonald *et al.*, 2009). Unsurprisingly, the relative standard deviations increase for lower elemental abundances, reflecting, at least partly,

the analytical imprecision. We note, however, the high values for ZrO₂ (Nettuno, 16%; Yellowstone, 27%) and ThO₂ (Nettuno, 11%; Yellowstone, 25%). The value for Nb₂O₅ for Nettuno is also high at 19%. These are outside

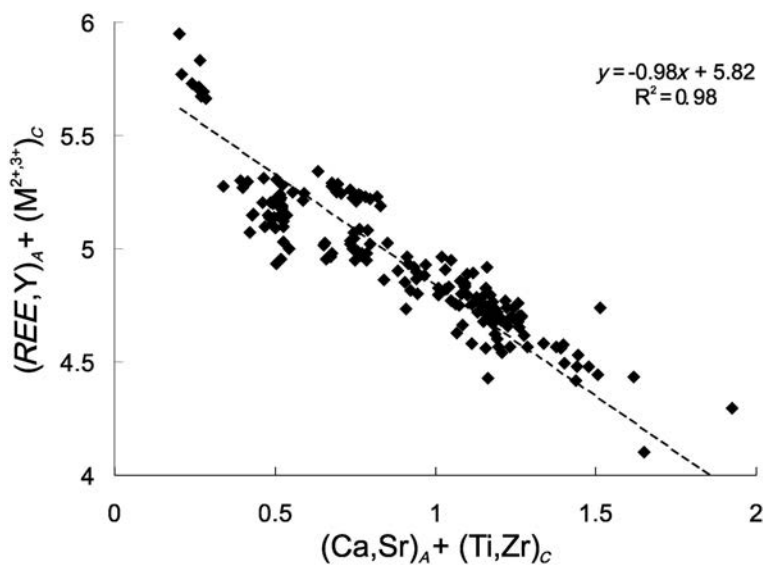


FIG. 4. Compositional variation in chevkinite-(Ce) from Russia and Mongolia can be satisfactorily represented by the scheme suggested by Vlach and Gualda (2007) in which $(Ca + Sr)_A + (Ti + Zr)_C \leftrightarrow [REE, Y]_A + (M^{2+}, M^{3+})_C$. Data are from Supplementary Table 1.

estimated relative precisions, 5–10% for oxide concentrations <1 wt.%. It would appear, therefore, that although these CGMs from erupted rocks are fairly homogeneous in terms of the major components, the minor components, especially the highly charged cations, can show significant intra-crystalline variation. This primary heterogeneity complicates the interpretation of heterogeneities resulting from secondary processes, such as metamictization and low-temperature hydrothermal alteration. Nonetheless, there is evidence from the Keivy samples of compositional changes that were probably produced by hydrothermal processes.

Hydrothermal alteration of chevkinite-group minerals

The chevkinite-(Ce) crystals in Keivy sample 1/93 are patchily mantled by a thin (up to 100 μm) zone of a dark material on back-scattered electron (BSE) images, and this is also present along cracks in the crystal interiors (Fig. 5*a,b*). The darker material has lower La, Ce, Pr, Nd and Fe contents and higher Ca, Th, U, Gd, Dy, Y, Ti, Al, Nb and Si contents than the lighter material (Supplementary Table 1*b,c*). Assuming CGM site allocations, there are low cation occupancies of the *B* site (as little as 0.29) and a very low overall

cation sum, with a mean of 12.3. The chevkinite-(Ce) in Keivy sample 160b/62 is rimmed (up to 70 μm thickness) and partially replaced by a material (Fig. 5*c,d*) that on BSE images appears grey and is therefore dissimilar to the altered material in sample 1/93. This material is, in turn, mantled by allanite-(Ce). The compositional changes are rather different to those in sample 1/93 (Supplementary Table 1*b,c*). Whereas *LREE* are slightly lower and Ti, Th and U enriched in the altered phase, Si is lower and FeO* shows little change. The cation sums, with a mean of 12.6, are lower than in fresh CGMs (ideally 13). We have no other information on the nature of the altered material, for example whether it constitutes a mineral that is not in the chevkinite group, or even a mixture of minerals.

Jiang (2006) reported altered chevkinite-(Ce) mantled by a corona of allanite-ilmenite-titanite-epidote-quartz in altered syenites from the Shuiquangou syenitic intrusion, northern China. During replacement of the chevkinite, some *REE* and Th was transported out of the mineral to be incorporated into allanite and titanite, whereas Si and Ti were essentially immobile. Vlach and Gualda (2007) documented increases in Ti, Th, U and Al, decreases in Fe, *REE* + Y, low analytical totals and poor-quality structural formulae in the altered zones that formed during alteration of

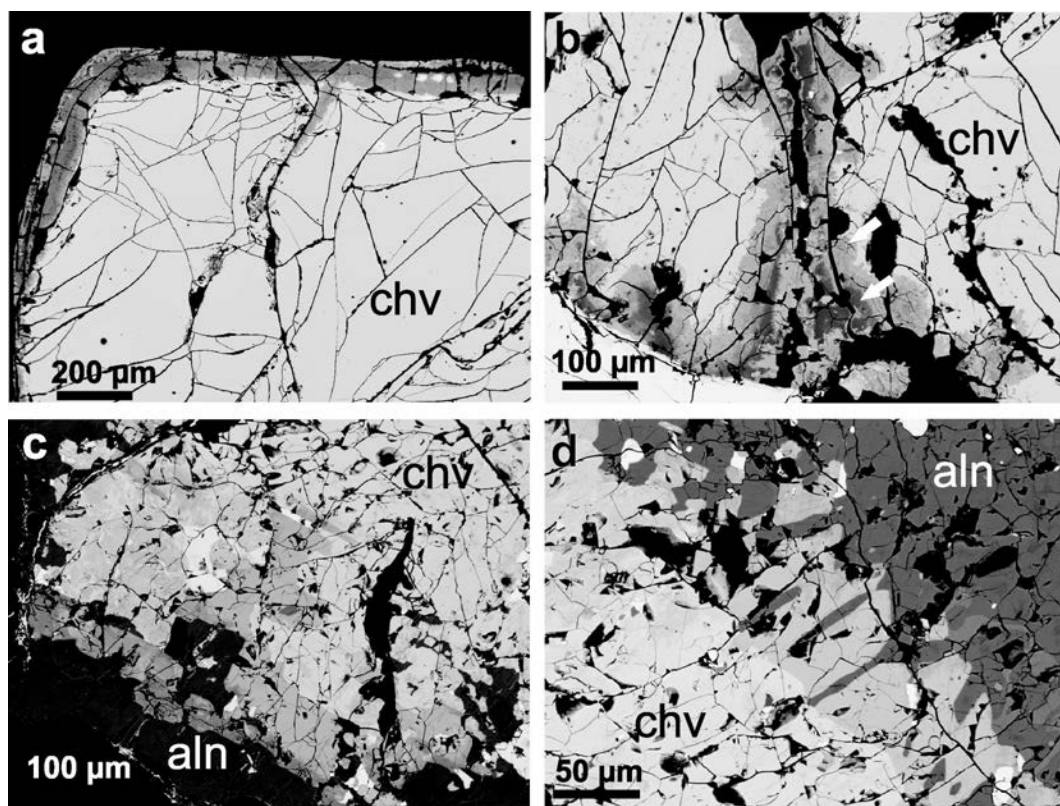


FIG. 5. Back-scattered electron (BSE) images of CGMs from the Keivy complex. (a) Fractured CGM (chv) mantled by thin rim of darker material which we interpret as a result of hydrothermal alteration (sample 1/93); (b) fractured CGMs replaced marginally and along cracks by hydrothermally altered material (arrowed) (sample 1/93); (c) CGMs (chv; brighter) rimmed and partially replaced by slightly darker, hydrothermally altered material, in turn mantled by allanite-(Ce) (aln; dark) (sample 160b/62); (d) CGMs rimmed by hydrothermally altered material, in turn mantled by allanite-(Ce). Note the fingers of allanite penetrating into the altered phase and stopping at the boundary with the CGM in this image of sample 160b/62.

chevkinite-(Ce) from the Graciosa Province, Brazil. In common with Jiang (2006), they ascribed the compositional changes to the interaction between magmatic chevkinite and hydrothermal fluids. The low analytical totals in the dark areas and their sharp boundaries with the lighter areas, which can be taken to mark the locations where chemical alteration along a progressing reaction front had stopped, are consistent with fluid-driven replacement reactions (Nasdala *et al.*, 2009). A similar origin by interaction with low-temperature fluids may reasonably be inferred for the Keivy examples, but the details of the chemical transfers in each sample, and in the Chinese and Brazilian

examples, are different, possibly in response to differences in fluid composition, intensive parameters, and the surrounding mineral assemblages, in that some minerals may be more reactive than others under given conditions.

Acknowledgements

Financial support came from University of Warsaw grant BST 1536/4 IGMiP-22-2011 and MNiSW grant N N307 634040 and from the Russian Foundation for Basic Research grant 03-05-64158. We gratefully acknowledge detailed and constructive reviews by Edward Grew, Pavel Uher and Silvio Vlach, which resulted in

considerable improvements to the original manuscript. We also thank Roger Mitchell for helpful editorial suggestions.

References

- Andreev, G.V. and Ripp, G.S. (1995) About perrierite found in apatite ore. *Proceedings of the Russian Mineralogical Society*, **124**, 83–84, [in Russian, with English abstract].
- Belkin, H.E., Macdonald, R. and Grew, E.S. (2009) Chevkinite-group minerals from granulite-facies metamorphic rocks and associated pegmatites of East Antarctica and South India. *Mineralogical Magazine*, **73**, 149–164.
- Carlier, G and Lorand, J.-P. (2008) Zr-rich accessory minerals (titanite, perrierite, zirconolite, baddeleyite) record strong oxidation associated with magma mixing in the south Peruvian potassic province. *Lithos*, **104**, 54–70.
- Chakhmouradian, A.R. and Mitchell, R.H. (1999) Primary, agpaitic and deuteric stages in the evolution of accessory Sr, REE, Ba and Nb-mineralization in nepheline-syenite pegmatites at Pegmatite Peak, Bearpaw Mountains, Montana. *Mineralogy and Petrology*, **67**, 85–110.
- Chukanov, N.V., Blaß, G., Pekov, I.V., Belakovsky, D.I., Rastsvetaeva, R.K. and Aksenov, S.M. (2011) Perrierite-(La), IMA 2010-089. CNMNC Newsletter No. 9, August 2011, page 2537; *Mineralogical Magazine*, **75**, 2535–2540.
- Gagnevin, D., Daly, J.S. and Kronz, A. (2010) Zircon texture and chemical composition as a guide to magmatic processes and mixing in a granitic environment and coeval volcanic system. *Contributions to Mineralogy and Petrology*, **159**, 579–596.
- Haggerty, S.E. and Mariano, A.N. (1983) Strontianloparite and strontio-chevkinite: two new minerals in rheomorphic fenites from the Paraná Basin carbonates, South America. *Contributions to Mineralogy and Petrology*, **84**, 365–381.
- Harlov, D.E. and Förster, H.-J. (2003) Fluid-induced nucleation of (Y+REE)-phosphate minerals within apatite: nature and experiment. Part II. Fluorapatite. *American Mineralogist*, **88**, 1209–1229.
- Ito, J. and Arem, J.E. (1971) Chevkinite and perrierite: synthesis, crystal growth and polymorphism. *American Mineralogist*, **56**, 307–319.
- Jarosewich, E. and Boatner, L. (1991) Rare-earth element reference samples for electron microprobe analysis. *Geostandards Newsletter*, **15**, 397–399.
- Jiang, N. (2006) Hydrothermal alteration of chevkinite-(Ce) in the Shuiquangou syenitic intrusion, northern China. *Chemical Geology*, **227**, 100–112.
- Kopylova, M.G., Rickard, R.S., Kleynstueber, A., Taylor, W.R., Gurney, J.J. and Daniels, L.R.M. (1997) First occurrence of strontian K-Cr-loparite and Cr-chevkinite in diamonds. *Russian Geology and Geophysics*, **38**, 405–420.
- Lumpkin, G.R. and Ewing, R.C. (1992) Geochemical alteration of pyrochlore group minerals: microlite subgroup. *American Mineralogist*, **77**, 179–188.
- Lumpkin, G.R. and Ewing, R.C. (1995) Geochemical alteration of pyrochlore group minerals: pyrochlore subgroup. *American Mineralogist*, **80**, 732–743.
- Lumpkin, G.R. and Ewing, R.C. (1996) Geochemical alteration of pyrochlore group minerals: betafite subgroup. *American Mineralogist*, **81**, 1237–1248.
- Macdonald, R. and Belkin, H.E. (2002) Compositional variation in minerals of the chevkinite group. *Mineralogical Magazine*, **66**, 1075–1098.
- Macdonald, R., Belkin, H.E., Wall, F. and Bagiński, B. (2009) Compositional variation in the chevkinite group: new data from igneous and metamorphic rocks. *Mineralogical Magazine*, **73**, 521–540.
- Miyajima, H., Matsubara, S., Miyawaki, R., Yokoyama, K. and Hirokawa, K. (2001) Rengeite, Sr₄ZrTi₄Si₄O₂₂, a new mineral, the Sr-Zr analogue of perrierite from the Itoigawa-Ohmi district, Niigata Prefecture, central Japan. *Mineralogical Magazine*, **65**, 111–120.
- Miyajima, H., Miyawaki, R. and Ito, K. (2002) Matsubaraitite, Sr₄Ti₅(Si₂O₇)₂O₈, a new mineral, the Sr-Ti analogue of perrierite in jadeitite from the Itoigawa-Ohmi district, Niigata Prefecture, Japan. *European Journal of Mineralogy*, **14**, 1119–1128.
- Nasdala, L., Kronz, A., Wirth, R., Váczi, T., Pérez-Soba, C., Willner, A. and Kennedy, A.K. (2009) The phenomenon of deficient electron microprobe totals in radiation-damaged and altered zircon. *Geochimica et Cosmochimica Acta*, **73**, 1637–1650.
- Nasdala, L., Hanchar, J.M., Rhede, D., Kennedy, A.K. and Váczi, T. (2010) Retention of uranium in complexly altered zircon: an example from Bancroft, Ontario. *Chemical Geology*, **269**, 290–300.
- Popov, V.A., Pautov, L.A., Sokolova, E., Hawthorne, F.C., McCammon, C. and Bazhenova, L.F. (2001) Polyakovite-(Ce), (REE,Ca)₄(Mg,Fe²⁺)(Cr³⁺,Fe³⁺)₂(Ti,Nb)₂Si₄O₂₂, a new metamict mineral species from the Ilmen Mountains, southern Urals, Russia: mineral description and crystal chemistry. *The Canadian Mineralogist*, **39**, 1095–1104.
- Portnov, A.M. (1964) Strontium perrierite in the North Baikal region. *Doklady of the Academy of Sciences USSR: Earth Sciences*, **156**, 118–120.
- Pouchou, J.L. and Pichoir, J.F. (1991) Quantitative analysis of homogeneous or stratified microvolumes applying the model 'PAP'. Pp. 31–75 in: *Electron Probe Quantitation* (H. Newbury, editor). Plenum Press, New York.

CHEVKINITE-GROUP MINERALS

- Ruschel, K., Nasdala, L., Rhede, D., Wirth, R., Lengauer, C.L. and Libowitzky, E. (2010) Chemical alteration patterns in metamict fergusonite. *European Journal of Mineralogy*, **22**, 425–433.
- Shen, G., Yang, G. and Xu, J. (2005) Maoniupingite-Ce: a new rare-earth mineral from the Maoniuping rare-earth deposit in Mianning, Sichuan. *Sedimentary Geology and Tethyan Geology*, **25**, 210–216.
- Shimazaki, H., Yang, Z., Miyawaki, R. and Shigeoka, M. (2008) Scandium-bearing minerals in the Bayan Obo Nb-REE-Fe deposit, Inner Mongolia. *Resource Geology*, **58**, 80–86.
- Tomašić, N., Gajović, A., Bermanec, V., Su, D.S., Rajić Linarić, M., Ntafos, T. and Schlögl, R. (2006) Recrystallization mechanisms of fergusonite from metamict mineral precursors. *Physics and Chemistry of Minerals*, **33**, 145–159.
- Townsend, K.J., Miller, C.F., D'Andrea, J.L., Ayers, J.C., Harrison, T.M. and Coath, C.D. (2000) Low temperature replacement of monazite in the Ireteba granite, Southern Nevada: geochronological implications. *Chemical Geology*, **172**, 95–112.
- Vlach, S.R.F. and Gualda, G.A.R. (2007) Allanite and chevkinite in A-type granites and syenites of the Graciosa Province, southern Brazil. *Lithos*, **97**, 98–121.
- Wang, R.U., Fontan, F., Chen, X.M., Hu, H., Liu, C.S., Xu, S.J. and de Parseval, P. (2003) Accessory minerals in the Xihuashan Y-enriched granitic complex, southern China: a record of magmatic and hydrothermal stages of evolution. *The Canadian Mineralogist*, **41**, 727–748.
- Xu, J., Yang, G., Li, G., Wu, Z. and Shen, G. (2008) Dingdaohengite-(Ce) from the Bayan Obo REE-Nb-Fe Mine, China: both a true polymorph of perrierite-(Ce) and a titanite analog at the C1 site of chevkinite subgroup. *American Mineralogist*, **93**, 740–744.
- Yang, Z., Ding, K., Giester, G. and Tillmanns, E. (2011) Hezuolinite, IMA 2010-045. CNMNC Newsletter No. 8, April 2011, page 289; *Mineralogical Magazine*, **75**, 289–294.
- Zozulya, D.R., Bayanova, T.B. and Eby, G.N. (2005) Geology and age of the Late Archean Keivy alkaline province, northeastern Baltic Shield. *Journal of Geology*, **113**, 601–608.

